Journal of Sound and Vibration (1998) **217**(4), 653–664
Article No. sv981763

OPTIMAL DYNAMIC ABSORBER FOR A ROTATING RAYLEIGH BEAM

MARKO JORKAMA

Valmet Winders, *Wärtsilänkatu* 100, *FIN*-04400 *Järvenpää*, *Finland*

AND

RAIMO VON HERTZEN

Laboratory of Theoretical and Applied Mechanics,
Helsinki University of Technology, *P.O. Box* 1100, *FIN*-02015 *HUT*, *Finland*

(*Received* 21 *November* 1997, *and in final form* 24 *March* 1998)

A theory of dynamic vibration absorbers for an elastically mounted rotating Rayleigh beam under a distributed load is presented. The novel features due to rotational motion are demonstrated via a numerical example of a paper machine roll with dynamic absorbers attached to the bearing houses. Depending on the horizontal to vertical bearing stiffness ratio, the optimal frequency response function may exhibit three peaks of equal height instead of the conventional two. It is also shown that the optimal values for absorber stiffness and damping depend significantly on the rotational speed of the beam and asymmetry of the bearing support. Finally, the effectiveness of the optimal absorber is analysed as a function of the absorber size and rotational speed.

© 1998 Academic Press

1. INTRODUCTION

The dynamic vibration absorber or simply dynamic absorber was invented at the beginning of the 20th century by Frahm [1], and since then, it has proven to be an indispensable device to reduce the undesirable vibrations in many applications such as gas turbines and engines, ship rolling, helicopters, electrical transmission lines etc. The discrete dynamic absorber was first analysed by Ormondroyd and Den Hartog [2], and the optimum damping was later derived by Brock [3]. Their studies covered a main system consisting of a mass and spring and a dynamic absorber with a mass, spring and viscous damper. For this system it was possible to obtain analytical expressions for the optimum tuning and damping of the absorber. Later, Thompson [4] extended the study to a viscously damped main system. He presented a numerical method, based on the frequency locus construction, for the determination of the optimum tuning and damping.

Young [5] was the first to consider the application of dynamic absorbers to beams. Snowdon [6] considered the optimization of the discrete absorber on beams with various boundary conditions when structural damping was present. Jacquot [7] used an approximate method in which the analogy established between a beam

0022–460X/98/440653 + 12 $30.00/0 © 1998 Academic Press

and a SDOF system allowed the use of the optimal absorber parameters for the latter to determine the ones for the beam. The main system damping was not included in his theory so that the analytical results of Den Hartog and Brock could be applied. Özgüven and Candir [8] extended Jacquot's treatment by considering a structurally damped beam with two dynamic absorbers for suppressing the first two resonances of the beam. A further extension was recently made by Manikanahally and Crocker [9] who included mounted rigid masses in their beam model.

The dynamics of rotating machinery constitute a comprehensive and important field of engineering applications. The previous works, however, do not account for the rotational motion of the beam. The gyroscopic coupling due to rotation connects the vertical and horizontal motions which, as will be shown, has a considerable effect on the optimal tuning and effectiveness of the absorber. In section 2 a general solution for the frequency response function of a uniform rotating Rayleigh beam is presented and the boundary conditions accounting for elastic supports and vertical dynamic absorbers are formed. Damping is included in both the main system and the absorbers. In section 3 the optimization procedure is considered. The optimization consists of minimizing the maximum of the frequency response function in the vicinity of the original resonance that is to be attenuated. In section 4 novel features in the optimal absorber design due to the rotational motion are demonstrated by studying an example of a paper machine roll with dynamic absorbers at its ends. The optimum tuning and damping for the absorbers are determined by solving the associated *min-max* problem numerically. Finally, the conclusions are drawn in section 5.

2. THEORY

The equations of motion of a uniform rotating Rayleigh beam (see Figure 1) can be written in the inertial co-ordinates as

$$\rho A\ddot{u} - \rho I\ddot{u}'' - 2\rho I\Omega\dot{v}'' + C_i(\dot{u} + \Omega v) + EIu'''' = f_u, \tag{1}$$

$$\rho A\ddot{v} - \rho I\ddot{v}'' + 2\rho I\Omega\dot{u}'' + C_i(\dot{v} - \Omega u) + EIv'''' = f_v, \tag{2}$$

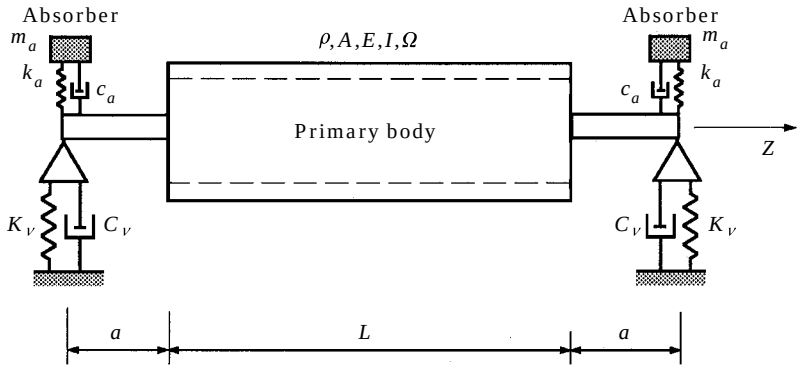

Figure 1. Spinning Rayleigh beam resting on springs and viscous dampers. The dynamic absorbers are also shown. The theory is developed for the limit $a \to 0$.

where $u(Z, t)$ and $v(Z, t)$ are the horizontal and vertical displacement fields, respectively, and $f_u(Z, t)$ and $f_v(Z, t)$ are the components of an external harmonic load. The density, cross-sectional area, moment of area, modulus of elasticity and rotational speed around the $+Z$-axis for the beam are ρ, A, I, E and Ω, respectively. The internal damping of the beam, proportional to the velocity of the beam relative to the rotating co-ordinate system, is accounted for by the viscous damping coefficient C_i. Under the harmonic load $f_u = \hat{f}_u\, e^{i\omega t}$ and $f_v = \hat{f}_v\, e^{i\omega t}$, the complex steady state amplitudes $\hat{u}(Z)$ and $\hat{v}(Z)$ are determined by the equations

$$\hat{u}'''' + \frac{\rho}{E}\omega^2\hat{u}'' - 2i\frac{\rho}{E}\Omega\omega\hat{v}'' - \frac{\rho A}{EI}\omega^2\hat{u} + i\frac{C_i}{EI}\omega\hat{u} + \frac{C_i}{EI}\Omega\hat{v} = \frac{1}{EI}\hat{f}_u, \tag{3}$$

$$\hat{v}'''' + \frac{\rho}{E}\omega^2\hat{v}'' + 2i\frac{\rho}{E}\Omega\omega\hat{u}'' - \frac{\rho A}{EI}\omega^2\hat{v} + i\frac{C_i}{EI}\omega\hat{v} - \frac{C_i}{EI}\Omega\hat{u} = \frac{1}{EI}\hat{f}_v, \tag{4}$$

where $i = \sqrt{-1}$ is the imaginary unit. The general solution of equations (3) and (4) can be shown to be

$$\hat{u}(Z) = \sum_{n=1}^{4} \{[A_n^- + g_n^-(Z)]\Phi_n^-(Z) + [A_n^+ + g_n^+(Z)]\Phi_n^+(Z)\}, \tag{5}$$

$$\hat{v}(Z) = i\sum_{n=1}^{4} \{[A_n^- + g_n^-(Z)]\Phi_n^-(Z) - [A_n^+ + g_n^+(Z)]\Phi_n^+(Z)\}, \tag{6}$$

where the basis functions are given by

$$\Phi_1^{\pm}(Z) = \sin \nu^{\pm} Z, \qquad \Phi_2^{\pm}(Z) = \cos \nu^{\pm} Z,$$
$$\Phi_3^{\pm}(Z) = \sinh \kappa^{\pm} Z, \qquad \Phi_4^{\pm}(Z) = \cosh \kappa^{\pm} Z, \tag{7}$$

the complex coefficients by

$$\nu^{\pm} = \sqrt{\frac{1}{2}\left\{\frac{\rho}{E}\omega(\omega \pm 2\Omega) + \sqrt{\left[\frac{\rho}{E}\omega(\omega \pm 2\Omega)\right]^2 + 4\frac{\rho A}{EI}\omega^2 - 4i\frac{C_i}{EI}(\omega \pm \Omega)}\right\}}, \tag{8}$$

$$\kappa^{\pm} = \sqrt{\frac{1}{2}\left\{-\frac{\rho}{E}\omega(\omega \pm 2\Omega) + \sqrt{\left[\frac{\rho}{E}\omega(\omega \pm 2\Omega)\right]^2 + 4\frac{\rho A}{EI}\omega^2 - 4i\frac{C_i}{EI}(\omega \pm \Omega)}\right\}}, \tag{9}$$

and the g-functions accounting for the load by

$$g_1^{\pm}(Z) = -\int_0^Z \frac{\hat{f}_u(z) \pm i\hat{f}_v(z)}{2EI\nu^{\pm}(\nu^{\pm 2} + \kappa^{\pm 2})} \cos \nu^{\pm} z \, dz, \tag{10}$$

$$g_2^{\pm}(Z) = \int_0^Z \frac{\hat{f}_u(z) \pm i\hat{f}_v(z)}{2EI\nu^{\pm}(\nu^{\pm 2} + \kappa^{\pm 2})} \sin \nu^{\pm} z \, dz, \tag{11}$$

$$g_3^{\pm}(Z) = \int_0^Z \frac{\hat{f}_u(z) \pm \mathrm{i}\hat{f}_v(z)}{2EI\kappa^{\pm}(v^{\pm^2} + \kappa^{\pm^2})} \cosh \kappa^{\pm} z \, \mathrm{d}z, \tag{12}$$

$$g_4^{\pm}(Z) = -\int_0^Z \frac{\hat{f}_u(z) \pm \mathrm{i}\hat{f}_v(z)}{2EI\kappa^{\pm}(v^{\pm^2} + \kappa^{\pm^2})} \sinh \kappa^{\pm} z \, \mathrm{d}z. \tag{13}$$

The boundary conditions of the problem are determined by the springs and dampers at the beam ends (see Figure 1) and the dynamic absorbers which here are assumed to execute vertical motion at the beam ends as well. The spring constants and viscous damping coefficients in the horizontal and vertical directions are K_u, C_u, K_v and C_v, respectively. The length of the beam is L. The steady state boundary conditions (14)–(21) and equations of motion for the absorbers (22) and (23) can be shown to be

$$EI\hat{u}'''(0) + \rho I\omega^2\hat{u}'(0) - 2\mathrm{i}\rho I\Omega\omega\hat{v}'(0) + (K_u + \mathrm{i}\omega C_u)\hat{u}(0) = 0, \tag{14}$$

$$EI\hat{v}'''(0) + \rho I\omega^2\hat{v}'(0) + 2\mathrm{i}\rho I\Omega\omega\hat{u}'(0) + (\mathscr{K}_v + \mathrm{i}\omega\mathscr{C}_v)\hat{v}(0) = (k_a + \mathrm{i}\omega c_a)\hat{V}_0, \tag{15}$$

$$\hat{u}''(0) = 0, \tag{16}$$

$$\hat{v}''(0) = 0, \tag{17}$$

$$EI\hat{u}'''(L) + \rho I\omega^2\hat{u}'(L) - 2\mathrm{i}\rho I\Omega\omega\hat{v}'(L) - (K_u + \mathrm{i}\omega C_u)\hat{u}(L) = 0, \tag{18}$$

$$-EI\hat{v}'''(L) - \rho I\omega^2\hat{v}'(L) - 2\mathrm{i}\rho I\Omega\omega\hat{u}'(L) + (\mathscr{K}_v + \mathrm{i}\omega\mathscr{C}_v)\hat{v}(L) = (k_a + \mathrm{i}\omega c_a)\hat{V}_L, \tag{19}$$

$$\hat{u}''(L) = 0, \tag{20}$$

$$\hat{v}''(L) = 0, \tag{21}$$

$$(k_a + \mathrm{i}\omega c_a - m_a\omega^2)\hat{V}_0 = (k_a + \mathrm{i}\omega c_a)\hat{v}(0), \tag{22}$$

$$(k_a + \mathrm{i}\omega c_a - m_a\omega^2)\hat{V}_L = (k_a + \mathrm{i}\omega c_a)\hat{v}(L), \tag{23}$$

where the notations

$$\mathscr{K}_v = K_v + k_a, \tag{24}$$

$$\mathscr{C}_v = C_v + c_a \tag{25}$$

have been used. Above m_a, c_a and k_a are the mass, damping coefficient and spring constant of the absorbers, and $\hat{V}_0$ and $\hat{V}_L$ the steady state amplitudes of the absorber displacements at the beam ends, respectively. The unknown coefficients $A_n^{\pm}$ ($n = 1, \ldots, 4$), $\hat{V}_0$ and $\hat{V}_L$ can be solved by substituting the solutions (5) and (6) into the equations (14)–(23). Although the above equations are restricted to the case of identical vertical absorbers, the analysis is general enough to provide a straightforward extension to the case of dissimilar absorbers in both vertical and horizontal directions.

Since the goal in the following is to suppress the beam response due to vertical load, the following case is considered:

$$\hat{f}_u = 0, \qquad \hat{f}_v = F(Z), \tag{26}$$

where the load function $F(Z)$ is normalized (in SI units) as

$$\|F\| = \sqrt{\frac{1}{L}\int_0^L |F(Z)|^2 \, \mathrm{d}Z} = 1. \tag{27}$$

The corresponding steady state solutions $\hat{u}(Z, \omega)$ and $\hat{v}(Z, \omega)$ are called the horizontal and vertical frequency response functions at Z, respectively.

3. OPTIMUM ABSORBER PARAMETERS

For non-rotating beams and discrete systems, the determination of the optimum absorber parameters is considered by several authors. The absence of damping in the main system has enabled authors to obtain closed form expressions for the optimum absorber parameters [3, 7]. The optimization procedure is based on the existence of two fixed points on the family of frequency response curves. The absorber is tuned so that the two fixed points represent equal amplitudes and the damping is selected as the average of the values rendering the response curve horizontal at either fixed point. If there is damping in the main system, the frequency response curves do not exhibit any fixed points. Thus the peak values of the response have to be examined. On the amplitude response surface $H = H(c, \omega)$, two separate saddle points will exist where the conditions $\partial H/\partial c = \partial H/\partial \omega = 0$ are satisfied. By careful selection of the absorber spring stiffness, these two saddle points may be adjusted to equal elevations and the average of the damping values corresponding to the saddle points are taken as the optimum [4]. Alternatively, the optimum parameters may be determined numerically by finding the values of the absorber tuning and damping which minimize the maximum of the response within a frequency range including the resonance to be suppressed. This min-max problem is solved by first finding the maximum of the two peaks (due to the absorber and original beam resonances) using a global maximization algorithm, and then by determining the tuning and damping values to minimize this maximum value [8]. That is, for a predetermined value of absorber mass, find $\min_{c_a,k_a} H_{\max}$, where

$$H_{\max}(c_a, k_a) = \max_{\omega \in I} H(\omega; c_a, k_a). \tag{28}$$

Here H denotes the amplitude response at a selected point of the beam and I an interval enclosing the frequency range concerned in the neighbourhood of the original resonance. It should be pointed out that the function $H_{\max}(c_a, k_a)$ is not differentiable at its minimum. In the vicinity of the optimal point (c_a, k_a), the saddle points of H are almost at equal elevations. Consequently, the particular saddle point which determines the value of the function $H_{\max}$ changes abruptly in the neighbourhood of the optimal point. Since the partial derivatives $\partial H/\partial c_a$ and $\partial H/\partial k_a$ are unequal for different saddle points, the function $H_{\max}$ develops a sharp edge or apex at the optimal point.

Let us now consider the case of a rotating beam with rotational speed Ω. Although any desired combination of the horizontal and vertical responses may be chosen as the objective function to be minimized, we consider in what follows

TABLE 1

Structural parameters used in the example

Parameter	Notation	Value
Modulus of elasticity	E	$2{\cdot}106 \times 10^{11}$ N m^{-2}
Cross sectional area	A	$0{\cdot}1257$ m^2
Roll density	ρ	7830 kg m^{-3}
Moment of area	I	$1{\cdot}010 \times 10^{-2}$ m^4
Vertical bearing stiffness	K_v	$6{\cdot}0 \times 10^8$ N m^{-1}
Horizontal and vertical bearing damping coefficients	C_u, C_v	$3{\cdot}94 \times 10^4$ Ns m^{-1}
Internal damping coefficient for the roll tube	C_i	$807{\cdot}65$ Ns m^{-2}
Absorber mass	m_a	300 kg

the case of a vertical objective function to illustrate the basic phenomena due to rotation, providing an easy comparison with earlier work on non-rotating beams. If the vertical harmonic load on the beam is represented by $\hat{f}_v = F(Z)$, where $\|F\| = 1$, the corresponding vertical frequency response function at a selected point is determined by $H = \hat{v}(\omega; c_a, k_a, \Omega)$. Due to the rotational motion, novel features in the response appear. Firstly, the frequency response function may exhibit (with respect to $\omega \in I$) three local maxima instead of one or two. Secondly, the number of maxima at equal elevations in the optimal situation, called here *primary maxima* (see section 4), may be one, two or three. For example, if the number of primary maxima is three, the surface $H_{\max}(c_a, k_a)$ takes the form of a tetrahedron standing on its apex and the contour lines constitute a set of nested triangles. Therefore, the optimal point cannot be found using numerical algorithms employing function gradients. We have successfully used the polytope method, which employs function values only. The method is based on function comparison and no smoothness is assumed. In the polytope method, a set of points on the surface (complex) moves down in an "amoeba-like fashion" towards the minimum point by taking steps in an adaptable manner [10].

4. APPLICATION

In order to illustrate the dependence of the optimal parameters of the dynamic absorbers on the rotational speed of the beam Ω, the present theory is applied to the case of a paper machine roll. We specify a harmonic vertical unit load on the roll by $\hat{f}_v = 1$ and calculate the corresponding response $\hat{v}(\omega; c_a, k_a, \Omega)$ at $L/2$, i.e., the vertical frequency response function at the centre of the roll. The parameter values used in the calculations are shown in Table 1. In the calculated examples below, we concentrate on the suppression of the lowest vertical beam resonance at 151 rad s^{-1}.

Let us consider the effect of the rotational speed Ω and the horizontal bearing stiffness K_u on the vertical frequency response function. Note that the gyroscopic coupling term in the horizontal equation of motion (1) is $-2\rho I\Omega\dot{v}''$, i.e., the larger the value of Ω the stronger the coupling. Under vertical harmonic forcing with a specified frequency, the quantity $\dot{v}''$ executes harmonic steady state oscillations

with the very same frequency. Since the frequency range of primary interest here lies in the neighbourhood of the lowest resonance frequency of the vertical beam motion, the amplitude of the horizontal response is determined, not only by Ω, but also by the location of the horizontal beam resonance with respect to the vertical one. When the horizontal and vertical resonances are close to each other, the energy transfer between these perpendicular directions becomes significant, leading to considerable changes in the optimal absorber parameter values. Note also that the horizontal motion couples back to the vertical motion via the term $2\rho I\Omega\dot{u}''$. Depending on the phase of this term relative to that of the vertical load f_v, the gyroscopic coupling may increase or decrease the vertical vibration amplitude.

In Figure 2 the vertical frequency response function at $L/2$ without the gyroscopic coupling term ($\Omega = 0$) is shown for the case of no dynamic absorbers and dynamic absorbers with $m_a = 300$ kg and optimum tuning and damping. The behaviour is similar to that of the analogous discrete systems [2] and non-rotating beams with absorbers [7, 8]: the original resonance peak is split into two (left and right) peaks of equal height on either side of the original one. The effect of Ω and K_u on the roll response can be seen in Figure 3(a)–(e) which display the vertical and horizontal frequency response functions at $L/2$ for five values of K_u each with three values of Ω. The corresponding horizontal resonance frequencies of the beam (without absorbers and gyroscopic coupling) are 145, 149, 151, 154 and 157 rad s^{-1}. In Figure 3(a) the horizontal resonance lies well below the vertical ones. The vertical load drives the horizontal motion via the gyroscopic coupling term leading to a maximum in the horizontal response close to the horizontal resonance frequency. At the same time, a decrease in the vertical amplitude occurs indicating that vibrational energy leaks from the vertical to the horizontal motion. This decrease (or *antiresonance*) is caused by a *destructive interference* of the external load and the gyroscopic coupling term $2\rho I\Omega\dot{u}''$ due to a steep change in the phase angle of u when traversing the horizontal resonance. As a result, the vertical frequency response function develops a minimum and, consequently, a

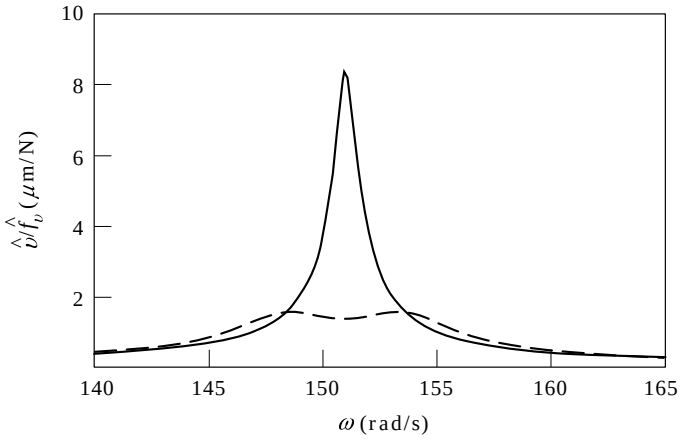

Figure 2. Vertical frequency response function at roll centre for the non-rotating beam in the case of no absorbers (solid line) and optimal absorbers with $m_a = 300$ kg (dashed line).

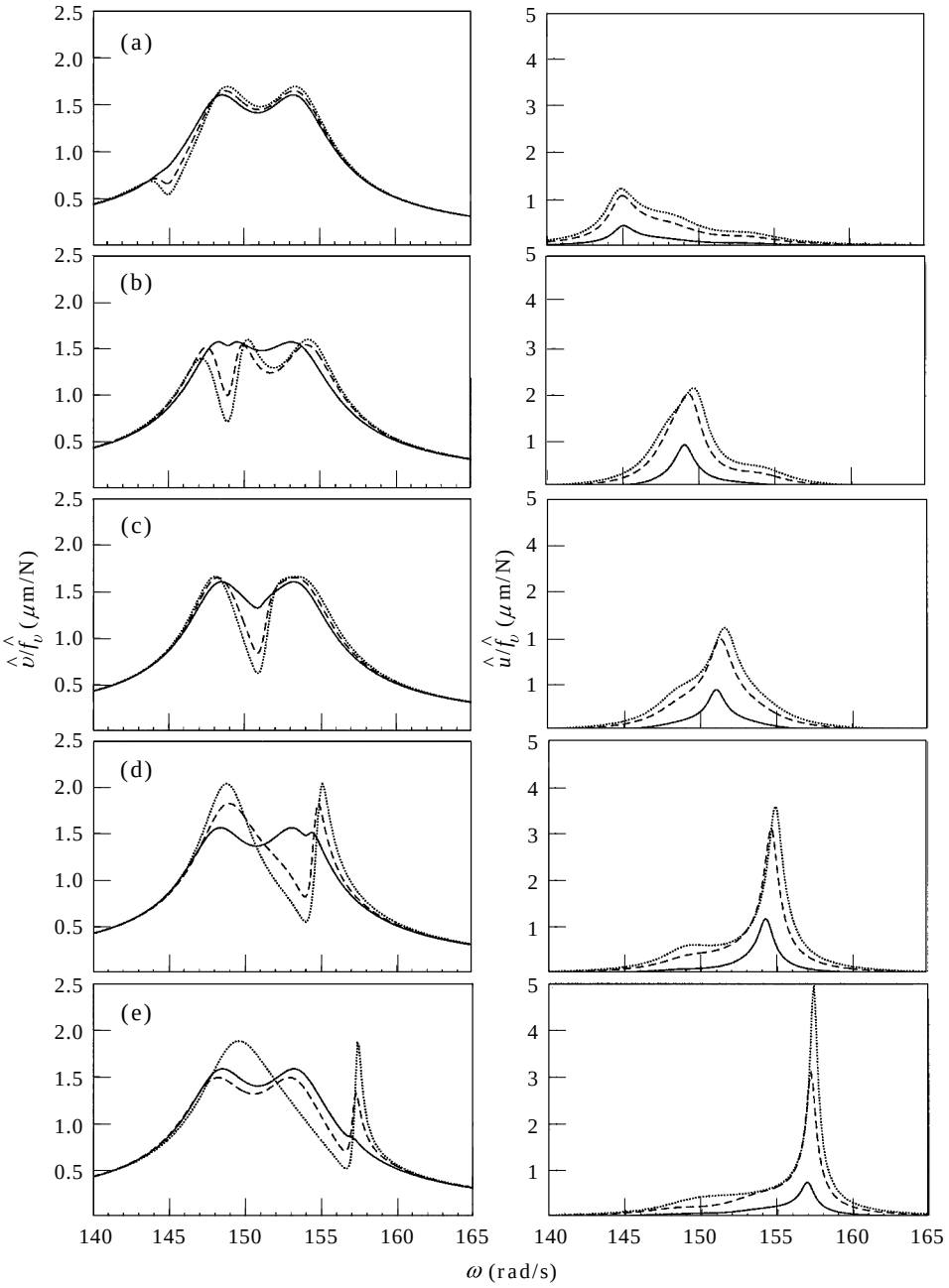

Figure 3. Development of the vertical and horizontal frequency response functions at roll centre for various values of K_u and Ω. The values of the horizontal to vertical bearing stiffness ratio are 64, 85, 100, 138 and 200% in (a)–(e), respectively. The values of Ω are 50, 160 and 220 rad s^{-1} (solid, dashed and dotted lines, respectively).

third maximum for sufficiently large values of Ω. However, this third maximum lies well below the two original ones and does not participate in the optimization procedure. For this reason we call this a *secondary maximum* whereas the two

others are called *primary maxima*. In Figure 3(b) the horizontal resonance has entered the region of the left vertical resonance. For $\Omega = 50$ rad s^{-1} all three maxima are primary whereas for $\Omega = 160$ and 220 rad s^{-1} only the two right ones are. This can easily be understood in terms of the deepening antiresonance. In Figure 3(c) the antiresonance occurs between the left and right vertical resonances. This leads to a further deepening of the minimum and no third maximum appears. In Figure 3(d) the horizontal resonance lies slightly above the right vertical resonance. For small Ω only a minor antiresonance can be seen and the two left maxima are primary. The increase of Ω suppresses the two right maxima developing a deep antiresonance. In this case, however, a strong new primary maximum appears due to the energy supply back from the horizontal to the vertical motion caused by a steep change in the phase angle of the gyroscopic term when the horizontal resonance is traversed (*constructive interference*). In Figure 3(e) the horizontal resonance lies well above the original vertical resonance. For $\Omega = 50$ rad s^{-1} the gyroscopic coupling is so small that the horizontal resonance hardly becomes visible in the vertical motion. However, when Ω becomes larger, the effect of the coupling increases significantly. For $\Omega = 160$ rad s^{-1} the third maximum is clearly visible although not yet a primary one. A moderate increase in Ω would lead to three primary maxima and a further increase in Ω suppresses the middle maximum leading to the case of two primary maxima as shown for $\Omega = 220$ rad s^{-1}.

The calculated optimal absorber parameters c_a and k_a as a function of the rotational speed for four values of K_u are shown in Figure 4. It can be seen that for 64% stiffness ratio the curves are smooth and almost independent of Ω. This behaviour is evident from Figure 3(a), since the horizontal resonance is far from the primary maxima and, therefore, the vertical motion is not affected by the gyroscopic coupling markedly. For 85% stiffness ratio the curves are non-smooth consisting of three smooth parts. The sharp corners occur at points where the number of primary maxima changes [see Figure 3(b)]. Also, the dependence of the optimal parameters on Ω is much stronger now. When the antiresonance occurs in the middle region between the original two maxima, as in the case of 100% stiffness ratio, only two primary maxima exist [see Figure 3(c)] and the optimal

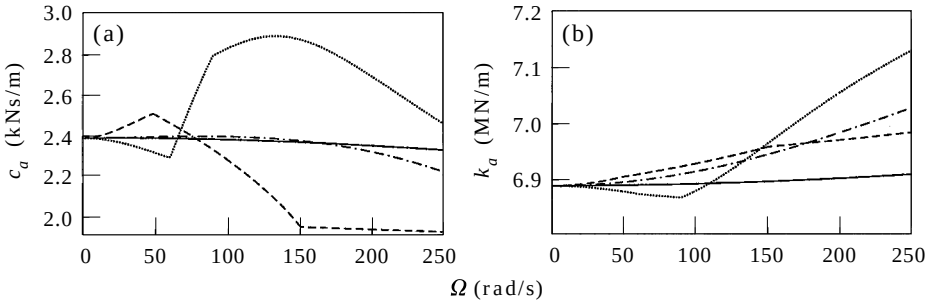

Figure 4. Optimal (a) damping coefficient c_a and (b) spring constant k_a for the absorbers as a function of the rotational speed Ω for 64, 85, 100 and 138% horizontal to vertical bearing stiffness ratios (solid, dashed, dashed-dotted and dotted lines, respectively).

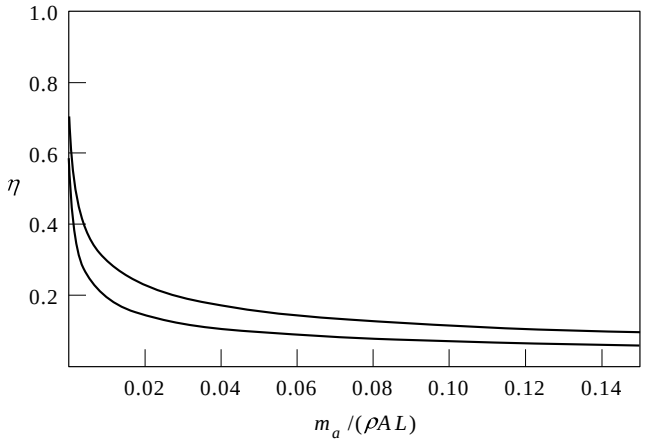

Figure 5. Amplitude reduction factor as a function of the absorber mass. The values of Ω are 0 and 220 rad s^{-1} (from top to bottom).

parameter curves are smooth. For 138% stiffness ratio the alternating primary maxima lead again to the non-smooth behaviour and strong Ω-dependence of the optimal curves. The corners occur at $\Omega = 60$ and 90 rad s^{-1}. Below 60 rad s^{-1} the two leftmost maxima are primary, between 60 and 90 rad s^{-1} all three are, and above 90 rad s^{-1} the two remaining ones are primary. Note that c_a exhibits a rapid rise already at 60 rad s^{-1} whereas k_a starts its rise at 90 rad s^{-1}. For still higher stiffness ratios the optimal curves remain qualitatively similar to the 138% case but are shifted to the right on the Ω-axis. The rapid growth in the curves, however, corresponding to the rise of the rightmost maximum to a primary one, is still enhanced and the corresponding humps become higher. For 300% stiffness ratio, for example, the optimal damping and tuning undergo in the range $0 < \Omega < 300$ rad s^{-1} altogether 91% and 7% relative changes, respectively. Note that c_a seems to be more sensitive to the gyroscopic coupling.

From a practical point of view the effectiveness of the absorber is of considerable interest. In order to study this, the *amplitude reduction factor* η will be defined as the ratio of the maximum value of the frequency response function (close to the lowest resonance) of the optimally tuned roll to that of the same roll without absorbers. The function η as a function of the absorber mass is plotted in Figure 5 for two values of Ω. The values of η fall steeply near the origin indicating that even small absorber masses lead to a considerable vibration attenuation. When the absorber mass increases further, η levels out and only a minor improvement is obtained. An increase in Ω leads to a considerable decrease in η since the resonance peaks without dynamic absorbers become higher due to the feedback mechanism caused by the gyroscopic coupling. The particularly good values of η in Figure 5 are partly due to the main system damping values which correspond to a lightly damped paper machine roll. However, even with heavily damped rolls, values of η around 30% can easily be achieved.

5. CONCLUSIONS

A closed form analytic solution for a rotating Rayleigh beam driven by an arbitrary harmonic load is presented. The boundary conditions are determined by horizontal and vertical translational springs, viscous dampers and vertical dynamic absorbers at the ends of the beam. The treatment of the field variables is general, however, and can be combined with any linear boundary conditions and additional dynamic absorbers as well. Due to the linearity of the problem the extension to an arbitrary time periodic load is also straightforward. From the optimization point of view, the present situation is more complex than the conventional one, where the optimization is based on the existence of two fixed points (no primary damping) [7] or two saddle points (with primary damping) [4]. Even so, a cost-effective calculation of the frequency response function is possible due to the analytical solution of the beam field equations. The optimization procedure for the dynamic absorbers in the present study is based on the *min-max* criterion of the vertical frequency response function.

As an application, a numerical example of a paper machine roll is studied. The significant effect of the gyroscopic coupling on the optimal absorber parameters, presented as a function of the rotational speed of the roll and bearing support asymmetry, is demonstrated. Three resonances of the non-rotating system, intimately coupled via the gyroscopic terms, play a role in the dynamic response. However, either two or three local maxima of the frequency response function are relevant (*primary*) in the optimization, contrary to the corresponding conventional cases with exactly two relevant maxima. The variation in the number of relevant maxima leads to a strong non-smooth dependence of the optimal absorber parameters on the rotational speed. The effectiveness of the dynamic absorber as a function of the absorber size is studied. The conclusion is that even for very small absorber masses, a considerable vibration attenuation can be achieved. The present theory can be utilized, for example, in suppressing nip induced vibrations in paper machinery.

Finally, it should be pointed out that a general load on the beam excites both the symmetrical and asymmetrical vertical modes of the beam-absorber system, which are then coupled with the horizontal motion. In our example the load was restricted to a symmetric one ($\hat{f}_v \equiv 1$) so that only the *absorbers-in-phase* with beam-in-phase or -antiphase vertical modes are excited. Further research should consider antisymmetric loads as well. The present study could also be extended by adding dynamic absorbers in the horizontal direction. This would further improve the amplitude reduction factor.

REFERENCES

1. H. Frahm 1909 *US Patent* No. 989 958. Device for damping vibrations of bodies.
2. J. Ormondroyd and J. P. Den Hartog 1928 *Transactions of the American Society of Mechanical Engineers Journal of Applied Mechanics* **49**, A9–A22. The theory of the dynamic vibration absorber.
3. J. E. Brock 1946 *Transactions of the American Society of Mechanical Engineers Journal of Applied Mechanics* **68**, A248. A note on the damped vibration absorber.

4. A. G. THOMPSON 1981 *Journal of Sound and Vibration* **77**, 403–415. Optimum tuning and damping of a dynamic vibration absorber applied to a force excited and damped primary system.
5. D. YOUNG 1952 *Proceedings of the First U.S. National Congress of Applied Mechanics*, 91–96. Theory of dynamic vibration absorbers for beams.
6. J. C. SNOWDON 1966 *Journal of the Acoustical Society of America* **39**, 878–886. Vibration of a cantilever to which dynamic absorbers are attached.
7. R. G. JACQUOT 1978 *Journal of Sound and Vibration* **60**, 535–542. Optimal dynamic vibration absorbers for general beam systems.
8. H. N. ÖZGÜVEN and B. CANDIR 1986 *Journal of Sound and Vibration* **111**, 377–390. Suppressing the first and second resonances of beams by dynamic vibration absorbers.
9. D. N. MANIKANAHALLY and M. J. CROCKER 1991 *Journal of Vibration and Acoustics* **113**, 116–122. Vibration absorbers for hysteretically damped mass-loaded beams.
10. P. E. GILL, W. MURRAY and M. H. WRIGHT 1981 *Practical Optimization*. New York: Academic Press.

APPENDIX: NOMENCLATURE

A	beam cross-sectional area
c_a	absorber damping coefficient
C_i	internal damping coefficient of the beam
C_u, C_v	horizontal and vertical bearing damping coefficients
$\mathscr{C}_v$	$C_v + c_a$
E	beam modulus of elasticity
f_u, f_v	horizontal and vertical loads
$\hat{f}_u, \hat{f}_v$	harmonic load amplitudes (complex)
H	amplitude response; frequency response function
$H_{\max}$	maximum of H with respect to ω
i	imaginary unit
I	beam moment of area
k_a	absorber spring stiffness
K_u, K_v	horizontal and vertical bearing stiffnesses
$\mathscr{K}_v$	$K_v + k_a$
L	beam length
m_a	absorber mass
u, v	horizontal and vertical beam centre line displacements
$\hat{u}, \hat{v}$	harmonic displacement amplitudes (complex)
$\hat{V}_0$, $\hat{V}_L$	harmonic absorber displacement amplitudes at beam ends (complex)
Z	co-ordinate along beam
η	amplitude reduction factor
ω	excitation frequency
Ω	beam angular velocity
ρ	beam density.